Rose Deformation Patterns in Thin Films Irradiated by Focused Laser Beams

J. Lauzeral,[1] D. Walgraef,[1,2] and N. M. Ghoniem[2]
[1]*Center for Nonlinear Phenomena and Complex Systems, Free University of Brussels, CP 231, Bd du Triomphe, B-1050 Brussels, Belgium*
[2]*Mechanical and Aerospace Engineering Department, The University of California at Los Angeles, Los Angeles, California 90024*
(Received 11 March 1997)

The coupling between surface deformation and defect dynamics may be at the origin of deformation patterns in thin films under laser irradiation. We analyze a simple model describing the dynamics of such systems in the case of focused laser irradiation. We show, through linear, nonlinear, and numerical analysis, how rose deformation patterns, with the petal number increasing with laser intensity, naturally arise in this model, in agreement with experimental observations. [S0031-9007(97)04173-2]

PACS numbers: 61.80.Az, 62.20.Fe, 68.45.Nj, 81.65.–b

Laser surface interaction is particularly important in technological applications where thin films, coatings, semiconductor surfaces, etc., play a leading role. Effectively, strong laser irradiation induces structural and morphological changes in matter which are responsible for the degradation of light emitting devices, the cumulative laser damage of optical components, and the nonuniform melting of semiconductor surfaces, to cite only a few of these aspects [1–3]. Laser annealing and fast recrystallization [4], as well as laser assisted thin film deposition processes, are also in the mainstream of this activity [5]. Furthermore, the fundamental nature of laser interaction with materials in industrial processes is recently highlighted in Ref. [6].

Many of these phenomena proceed through the formation of regular structures on the surface of the materials. For example, in the case of thin films under laser irradiation, regular deformation patterns may appear on the film surface when the laser intensity exceeds some threshold. In spatially extended irradiation zones, one- and two-dimensional gratings have been widely observed [7,8]. On the other hand, when irradiation proceeds with focused beams, such as in laser induced film deposition [9] or in etching experiments [10], roselike deformation patterns are observed, where a finite number of petals develop around a central uniform spot. Our aim in this Letter is to show that these patterns naturally appear in a dynamical model, introduced by Emel'yanov [9], which describes the evolution of the relevant physical variables for the destabilization of deformation-free surfaces.

The main instability mechanism in laser irradiated materials is due to the coupling between defect dynamics and surface deformation [9]. Effectively, on the one hand, strong laser irradiation generates an excess of defects in the surface layer. Example are electron-hole pairs in strongly absorbing semiconductors, voids or dislocation loops in prolonged irradiation, interstitial or vacancies in thin film deposition, coating, and laser annealing. On the other hand, the defect field gives rise to strong deformations of the subsurface layer of the material. Finally, it is the coupling between defect generation, diffusion, and deformation fields which leads to pattern forming instabilities. The dynamical description of such phenomena has thus to be based on the dynamics of the defect field N_d in the layer and the elastic continuum of the host material described by the displacement vector $\vec{\mathrm{U}}(\mathbf{r}, t)$, both dynamics being coupled through the defect-strain interaction.

In this Letter, we will consider laser induced deformation of thin films with weak adhesive forces to the substrate ($\leq$10 MPa), in comparison to the transverse vacancy body force ($\simeq$100 MPa). In this case, the evolution of the system is governed by the interaction between the bending of the film and the vacancy density, N_v, which is created in the layer as the result of thermal heating induced by laser irradiation. The evolution of the vacancy density is described by the following kinetic equation [9,11,12]:

$$\begin{aligned}\partial_t N_v = {} & D_\perp \partial_{zz}^2 N_v + D_\parallel \triangle N_v - \frac{N_v}{\tau} \\ & - \vec{\nabla}\left(\frac{\theta_v N_v D_\parallel}{kT}\right) \cdot \vec{\nabla}(\vec{\nabla} \cdot \vec{\mathrm{U}}) \\ & + g \exp\left(-\frac{E_v - \theta_v \vec{\nabla} \cdot \vec{\mathrm{U}}}{kT}\right). \end{aligned} \tag{1}$$

The film is horizontal and irradiated from above. Its midplane is characterized by the vertical coordinate $z = 0$ and the upper and lower surfaces are determined by $z = +h/2$ and $z = -h/2$, respectively. Furthermore, $\triangle = \partial_{xx}^2 + \partial_{yy}^2$, and $\vec{\nabla} = \vec{1}_x \partial_x + \vec{1}_y \partial_y$.

This evolution is triggered by vacancy generation ($E_v - \theta_v \vec{\nabla} \cdot \vec{\mathrm{U}}$ is the defect formation energy in a strained crystal, and g is the entropy of vacancy generation, $g \simeq 1$), annihilation (τ is the mean vacancy lifetime), and mobility. The latter is due to diffusion ($D_\perp$ is the transverse component of the diffusion tensor and $D_\parallel$ is its in-plane component), and to the extra defect flux, $\vec{\mathrm{J}} = -\frac{\theta_v N_v D_\parallel}{kT} \vec{\nabla}(\vec{\nabla} \cdot \vec{\mathrm{U}})$ induced by the layer deformation ($\theta_v = -0.2 b^3 K$ is the elastic interaction energy per vacancy, K is the bulk elastic modulus, and b is the Burger's vector).

 0031-9007/97/79(14)/2706(4)$10.00

The second part of the dynamics is described by the evolution of the film bending coordinate ζ, which measures the displacements along the z axis of the midlayer points. The strain-bending coupling is described by the relation

$$\vec{\nabla} \cdot \vec{\mathrm{U}} = -z\gamma \triangle_{\|} \zeta \,, \tag{2}$$

with $\gamma = (1 - 2\nu)/(1 - \nu)$, where ν is the Poisson coefficient of the film.

The equation of motion for the elastic film, expressed in terms of the bending coordinate ζ, is given by its elastic response to the transverse force acting on the film. The transverse adhesion forces are neglected in comparison to the body force due to vacancy strain energy gradients. It may then be written as [13]

$$\partial_t^2 \zeta + \frac{c^2 h^2}{12} \triangle_{\|}^2 \zeta - \frac{1}{\rho} \sigma_{ij} \partial_{ij}^2 \zeta = -\frac{\theta_v}{\rho h} \int_{-h/2}^{h/2} \partial_z N_v \,, \tag{3}$$

where σ_{ij} are the in-plane stress tensor components, induced by the stretching of the film, and where the usual tensor index notation and summation convention is used. c is the velocity of sound, h is the layer thickness, and ρ is its mass density. In usual experimental conditions [9], $D_{\|}\tau \simeq 10^{-5}$ cm^2, $\theta_v \simeq 10^{-10}$ erg, and $c \simeq 10^5$ cm s^1.

The linear stability analysis of this dynamical system shows, under uniform irradiation conditions, the occurrence of a pattern forming instability when the vacancy density exceeds a well-defined threshold [9,11]. In focused cw laser irradiation, however, laser spots with Gaussian axis-symmetric intensity profiles increase only locally the temperature of the film, as extensively discussed in [5]. At the surface, it acquires the following spatial dependence [9]:

$$\begin{aligned} T(\vec{\mathrm{r}}, h/2) &= T_0 + (T_S - T_0) \exp\left(-\frac{r^2}{r_0^2}\right) \\ &= T_+(r) \,, \end{aligned} \tag{4}$$

with $T_S - T_0 \simeq P(1 - R)/\sqrt{2\pi}\,\kappa(T_0) r_0$ [5], where P is the laser power, R is the reflectivity of the film and $\kappa(T_0)$ is its thermal conductivity (for example, for Mo/glass films irradiated by 488 nm Ar^+ cw 16 μm wide laser spots, $T_S - T_0 \simeq 10^4 P$, with P expressed in mW [10]).

In this case, the basic state, in the absence of deformation, is not horizontally uniform, and the corresponding vacancy density on the upper surface, $N_+(\vec{\mathrm{r}}) = N_v^0(\vec{\mathrm{r}}, h/2)$, is determined by the steady state of the equation,

$$\partial_t N_+(\vec{\mathrm{r}}) = D_{\|} \triangle N_+(\vec{\mathrm{r}}) - \frac{1}{\tau} [N_+(\vec{\mathrm{r}}) - G_+(r)] \,, \tag{5}$$

where $G_+(r)$ behaves as

$$G_+(r) = N_0 + (N_S - N_0) \exp\left(-\frac{r^2}{r_1^2}\right) \tag{6}$$

with $N_S = g\tau \exp(-E_v/kT_S)$, $N_0 = g\tau \exp(-E_v/kT_0)$, and $r_1 \simeq \sqrt{kT_S/E_v}\, r_0$ [9]. The defect density in the lower surface, $N_-(\vec{\mathrm{r}})$, is determined by the same method, but by taking into account that the temperature is reduced, according to the film thickness and thermal conductivity [5].

On defining the perturbations of the undeformed state as $n_\pm(\vec{\mathrm{r}}, t) = N_v(\vec{\mathrm{r}}, \pm h/2, t) - N_\pm(r)$, and performing the following scalings,

$$\begin{aligned} &\partial_t = \frac{1}{\tau} \partial_T, \qquad \triangle = \frac{\triangle}{\tau D_{\|}}, \qquad \alpha = \frac{6\nu\theta_v^2 D_{\|}\tau}{\rho c^2 h^2 k} \,, \\ &\xi = \frac{h\nu \parallel \theta_v \parallel}{2kD_{\|}\tau} \zeta \,, \\ &N = \alpha(n_+ + n_-), \qquad n = \alpha(n_+ - n_-) \,, \\ &\mu = \alpha\left(\frac{N_+}{T_+} + \frac{N_-}{T_-}\right), \\ &\eta = \alpha\left(\frac{N_+}{T_+} - \frac{N_-}{T_-}\right), \qquad \kappa = \frac{T_+ + T_-}{2T_+T_-} \,, \\ &\delta = \frac{T_+ - T_-}{2T_+T_-} \,, \end{aligned} \tag{7}$$

the dynamical model may be rewritten as

$$\begin{aligned} \partial_T N &= \triangle N - N - \vec{\nabla}\eta \cdot \vec{\nabla}(\triangle + 1)\xi \\ &\quad - \vec{\nabla}(\kappa n + \delta N) \cdot \vec{\nabla}\triangle\xi \,, \\ \partial_T n &= \triangle n - n - \vec{\nabla}\mu \cdot \vec{\nabla}(\triangle + 1)\xi \\ &\quad - \vec{\nabla}(\kappa N + \delta n) \cdot \vec{\nabla}\triangle\xi \,, \\ \frac{1}{\beta^2} \partial_T^2 \xi &= -\triangle^2 \xi - u\sigma_{ij}(\xi) \partial_{ij}^2 \xi - n \,, \end{aligned} \tag{8}$$

where the parameters μ, η, κ, and δ are space dependent, and where $u = 6(\frac{2kTD_{\|}\tau}{\theta_v h^2 \nu})^2$, $\beta = ch/D_{\|}\sqrt{12}$.

The input parameters to this model are ν, c, ρ, θ_v, $D_\perp$, $D_{\|}$, E_v, g, and τ. Of these nine parameters, only the vacancy mean lifetime is adjustable, because it depends on the film microstructure. The other eight parameters can be evaluated from basic materials data, at least in principle.

It is the parameter μ that here plays the role of the bifurcation parameter. It combines the spatial variation of the vacancy density and temperature profiles. Contrary to the approximation made in [9], $D_{\|}\tau \geq r_1^2$, and the spatial extension of the vacancy density is wider than that of the temperature. As a result, $\mu(r)$ acquires a crater shape, as can be seen in Fig. 1.

The natural patterns which are compatible with this geometry correspond to linear combinations of the eigenfunctions of the circle, i.e., to the functions $J_m(qR)\, \exp \pm im\phi$. Hence, linear and nonlinear analysis of this problem may be performed through expansions of the dynamical variables on Bessel functions of increasing order, in analogy with the theoretical analysis of the Bénard-Marangoni convection in small cylindrical containers [14,15], where pattern formation phenomena presents striking similarities with the ones described in this Letter [16].

The linear stability analysis of the undeformed basic state is thus performed on expressing defect and

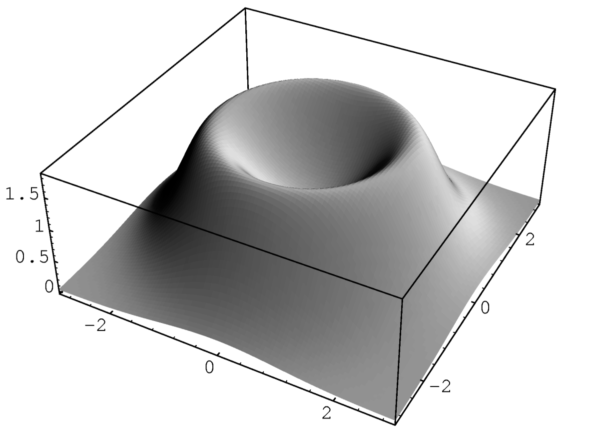

FIG. 1. Spatial dependence of the reduced bifurcation parameter $\mu(r)/\mu(0)$ obtained from Eqs. (5) and (6), with $N_S/N_0 = 350$, $T_S/T_0 = 4$, and $r_1 = 1.5r_0$.

deformation fields as

$$\begin{Bmatrix} n \\ N \\ \xi \end{Bmatrix} = \sum_{mi} \left(\begin{Bmatrix} n_{mi} \\ N_{mi} \\ \xi_{mi} \end{Bmatrix} e^{im\phi} + \text{c.c.} \right) J_m(k_{mi}R) , \tag{9}$$

and on linearizing their dynamics. $m = 0, 1, 2, \dots$ is the azimuthal wave number, J_m is the Bessel function of order m, and i is the radial wave number, which indexes the values k_{mi} satisfying the boundary condition $J_m(ka_0) = 0$. In the Bénard-Marangoni problem, a_0 corresponds to the radius of the vessel, but in our case we do not have such a sharp boundary condition. Nevertheless, due to the Gaussian decay of the bifurcation parameter on space scales of order r_1, one may safely choose values of k_{mi} satisfying the condition $J_m(ka_0) = 0$, with $a_0 \simeq 10R_1$, to perform the analysis, and the linearized dynamics becomes

$$\begin{aligned} \partial_T N_{mi} &= -(1 + k_{mi}^2) N_{mi} + (k_{mj}^2 - 1) \\ &\quad \times [(k_{mj}^2 + k_{mi}^2)\eta_{ij}^{(m)} + (\triangle\eta)_{ij}^{(m)}]\xi_{mj} , \\ \partial_T n_{mi} &= -(1 + k_{mi}^2) n_{mi} + (k_{mj}^2 - 1) \\ &\quad \times [(k_{mj}^2 + k_{mi}^2)\mu_{ij}^{(m)} + (\triangle\mu)_{ij}^{(m)}]\xi_{mj} , \\ \frac{1}{\beta^2}\, \partial_T^2 \xi_{mi} &= -k_{mi}^4 \xi_{mi} - n_{mi} , \end{aligned} \tag{10}$$

where

$$\mu_{ij}^{(m)} = \frac{\int_0^1 dRRJ_m(k_{mi}R)\mu(R)J_m(k_{mj}R)}{[J_m'(k_{mi})]^2} , \tag{11}$$

and similar definitions hold for $(\triangle\mu)_{ij}^{(m)}$, $\eta_{ij}^{(m)}$, and $(\triangle\eta)_{ij}^{(m)}$.

Since $\beta \gg 1$, ξ may be adiabatically eliminated, and it is a matter of algebra to show that instability occurs when at least one eigenvalue of the following matrix,

$$\left(\frac{k_{mj}^2 - 1}{k_{mj}^4} [(k_{mj}^2 + k_{mi}^2)\mu_{ij}^{(m)} + (\triangle\mu)_{ij}^{(m)}] - (1 + k_{mi}^2)\delta_{ij}^{Kr} \right), \tag{12}$$

vanishes.

This gives us a set of marginal stability curves $\frac{N_S}{N_0} = f_m(\lambda, R_1)$, where λ stands for the materials parameters. Hence, the instability threshold corresponds to the minimum of these curves, which gives, for each value of R_1 and λ, the critical value of $\frac{N_S}{N_0}$ and of the azimuthal wave number, as represented in Fig. 2.

A weakly nonlinear analysis may be performed on expanding the deformation and defect fields in terms of the eigenmodes of the linear evolution matrix (12), which leads to an infinite system of ordinary differential equations (ODE's) for their amplitudes. This system may then be reduced to the evolution equations of the amplitudes of the unstable modes only, as a consequence of the center manifold theorem. The corresponding amplitude equations are of the Landau type, as in convection problems [14,15].

However, we have integrated numerically the complete dynamical system (8) in the limit $\beta \to \infty$, with $\eta = \delta = 0$ and $u \ll 1$, for increasing temperatures in the irradiation spot. Rose deformation patterns develop spontaneously and the number of petals increase with temperature, as predicted by the linear stability analysis. As shown in Fig. 3, the deformation patterns develop around an undeformed central spot, where the vacancy density is maximum.

It has to be noted that, in a real experiment, the parameters μ_0 and R_1 are linked since they both depend on the temperature of the laser spot. As a result, when the laser intensity increases, the state of the system describes a curve in the (μ_0, r_{eff}) plane, and instability occurs when this curve hits the marginal stability curve (cf. Fig. 2). In the conditions of our numerical experiment,

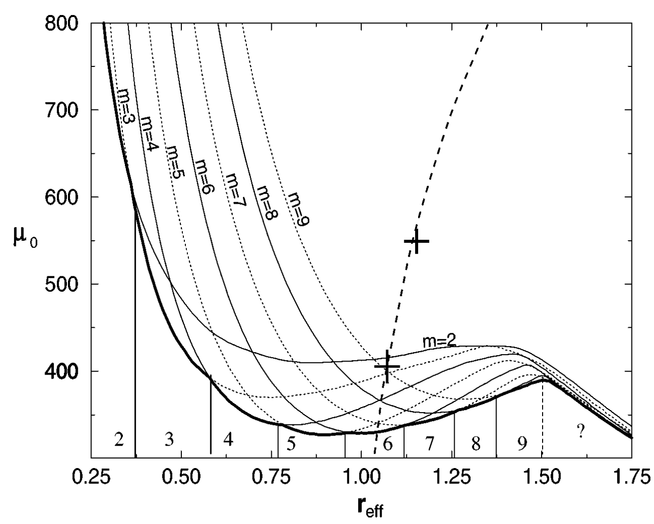

FIG. 2. Marginal stability curve in the ($\mu_0 = N_S/N_0$, $r_{\text{eff}} = R_1$) plane, where m is the azimuthal wave number. The dashed line represents the system's state and the selected azimuthal wave numbers are displayed above the r_{eff} axis. The crosses correspond to the simulations presented in Fig. 3.

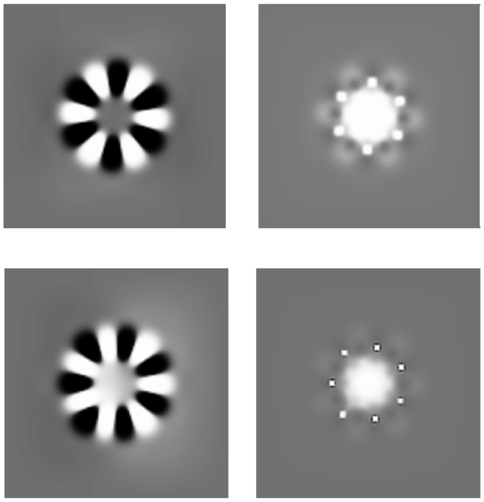

FIG. 3. Deformation field (left) and upper surface defect density (right) obtained by numerical integration of the system (8), for $\alpha N_0/T_0 = 1$, for a defect nucleation energy $E_v \simeq 0.35$ eV and for an irradiation spot radius $r_0 \simeq 20\ \mu$m. The upper set of graphs corresponds to $T_S \simeq 10^3$ °C (or $P \simeq 95$ mW), and the lower set corresponds to $T_S \simeq 1.2 \times 10^3$ °C (or $P \simeq 115$ mW).

instability occurs for $m = 6$ and $r_{\rm eff} \simeq 1$ (which corresponds to a laser power of $\simeq$85 mW in conditions where $T_S - T_0 \simeq 10^4 P$). Patterns with $m = 6$ should then appear for laser powers up to $\simeq$100 mW, while patterns with $m = 7$ should appear for powers between $\simeq$100 and $\simeq$130 mW, and patterns with $m = 8$ should appear for powers between $\simeq$130 and $\simeq$170 mW, in basic agreement with experimental observations [9,10]. For powers higher than $\simeq$195 mW ($r_{\rm eff} \simeq 1.5$), the structure of the pattern is expected to become ill defined since many modes become almost simultaneously unstable.

We have thus shown that the main aspects of deformation pattern formation in thin films irradiated with focused laser beams may be reproduced by a simple dynamical model based on the interaction between vacancy production and mobility and the film deformation field. In this context, the formation of roselike patterns is a natural consequence of the resulting instability mechanism in this specific geometry. In particular, the crater profile of the bifurcation parameter is a key element in understanding the shape of these patterns. It is crucially related to the fact that vacancies, although dominantly created in the center of the spot, diffuse away where they eventually annihilate. As a result, their concentration is maximum on a circle, and the undeformed state is unstable in a circular shell, where the pattern develops, in agreement with experimental observations.

The analysis presented here is in basic agreement with the experiments of Mogyorosi *et al.* [10]. However, more quantitative comparisons with specially designed experiments can be devised on the basis of this work. A better understanding and control of the mechanical behavior of thin films and surfaces under focused laser irradiation can thus be achieved. Deformation and failure of thin films are of growing interest in various areas of technological importance related to laser induced surface modification techniques [6] and possibly other techniques which include rapid heating of surfaces [17].

Financial assistance through NATO grant CRG-960490 is gratefully acknowledged. D. W. is supported by the Belgian National Fund for Scientific Research.

[1] *Surface Engineering, Surface Modification of Materials*, edited by R. Kossowsky and S. C. Singhal (Martinus Nijhoff, Dordrecht, 1984).
[2] *Interfaces under Laser Irradiation*, edited by L. Laude, D. Baeuerle, and M. Wautelet (Martinus Nijhoff, Dordrecht, 1987).
[3] *Science and Technology of Thin Film Superconductors*, edited by R. McConnell and R. Noufi (Plenum, New York, 1990).
[4] J. S. Preston, J. E. Sipe, and H. M. van Driel, in *Interfaces under Laser Irradiation*, edited by L. Laude, D. Bauerle, and M. Wautelet (Martinus Nijhoff, Dordrecht, 1987), pp. 127–136.
[5] D. Bauerle, *Chemical Processing with Lasers*, Springer Series in Materials Science Vol. 1 (Springer-Verlag, Berlin, 1986).
[6] D. Bauerle, *Laser Processing and Chemistry* (Springer-Verlag, New York, 1996).
[7] A. F. Banishev, V. I. Emel'yanov, and M. M. Novikov, Laser Phys. **2**, 192 (1992).
[8] J. F. Young, J. S. Preston, and H. M. van Driel, Phys. Rev. B **27**, 1141 (1983); **27**, 1155 (1983).
[9] V. I. Emel'yanov, Laser Phys. **2**, 389 (1992).
[10] P. Mogyorosi, K. Piglmayer, and D. Bauerle, Surf. Sci. **208**, 232 (1989).
[11] D. Walgraef and N. M. Ghoniem, "An Investigation of Laser-induced Deformational Instabilities in Thin Films," Proceedings of the 6th International Workshop on Instabilities and Nonequilibrium Structures, Valparaiso, Chile (to be published).
[12] N. M. Ghoniem, J. Lauzeral, and D. Walgraef, "Deformation Patterns in Thin Films under Uniform Laser Irradiation" (to be published).
[13] L. D. Landau, *Theory of Elasticity* (Pergamon Press, Oxford, 1986), 3rd ed.
[14] S. Rosenblat, S. H. Davis, and G. M. Homsy, J. Fluid Mech. **120**, 91 (1982).
[15] B. Echebarría, D. Krmpotić, and C. Pérez-García, Physica (Amsterdam) **99D**, 487 (1997).
[16] T. Ondarcuhu, J. Millán, H. L. Mancini, A. Garcimartín, and C. Pérez-García, Phys. Rev. E **48**, 1051 (1993).
[17] V. I. Emel'yanov and V. Y. Panchenko, *Nonlinear Optics of Low-Dimensional Structures and New Materials* (The International Society for Optical Engineering, Bellingham, Washington, 1996), Vol. 2801.